

# Results from the Multiwavelength Survey by Yale-Chile (MUSYC)

Ezequiel Treister<sup>1</sup>  
Eric Gawiser<sup>2</sup>  
Pieter Van Dokkum<sup>3</sup>  
Paulina Lira<sup>4</sup>  
Meg Urry<sup>3</sup>  
and the MUSYC Collaboration

<sup>1</sup> ESO

<sup>2</sup> Rutgers, State University of New Jersey, Piscataway, New Jersey, USA

<sup>3</sup> Yale University, New Haven, Connecticut, USA

<sup>4</sup> Universidad de Chile, Santiago de Chile, Chile

We present results from the MUSYC survey, which images a total of 1.2 square degrees spread over four fields in *UBVRiz'K* down to the spectroscopic limit,  $R \sim 25$ ,  $K \sim 22$  (AB). A significant fraction of the survey area has also been imaged by Chandra, XMM, GALEX, HST-ACS, near-infrared (JH), Spitzer-IRAC+MIPS, VLA, and ATCA. The main goals of this survey include the study of galaxy formation and evolution, Active Galactic Nuclei (AGN) and Galactic structure.

## The MUSYC survey

In recent years, extragalactic astronomy at high redshift has been dominated by deep multi-wavelength surveys. Examples of these surveys are the Hubble Deep Fields and the Great Observatories Origins Deep Survey (GOODS). These are very deep surveys over a relatively narrow area of the sky,  $\sim 0.2$  square degrees or less. These surveys allow us to study sources dimmer than the spectroscopic limit but suffer from significant sample variance, motivating a new generation of wider-area deep surveys that bridge the gap between HDF/GOODS and the shallower wide coverage of the Sloan Digital Sky Survey. The wide/deep surveys allow us to study a fair sample of the Universe at all redshifts  $z > 0.5$  and to

detect a statistically significant population of the brighter, and thus rarer, sources. Examples include Galaxy Evolution from Morphology and SEDs (GEMS), the VLT-VIRMOS Deep Survey (VVDS), the Cosmic Evolution Survey (COSMOS), the Deep Extragalactic Evolutionary Probe (DEEP-2), the NOAO Deep-Wide Field Survey (NDWFS), and the Multiwavelength Survey by Yale-Chile (MUSYC).

MUSYC is unique among the current generation of wide-deep surveys in having been optimised for the study of the high-redshift ( $z > 3$ ) Universe. This is achieved by imaging 1.2 square degrees spread over four fields down to the spectroscopic limit for modern 8-metre telescopes with coverage from *U*-band through *K*-band, in order to trace both the Lyman and Balmer/4000 Å breaks at  $z \sim 3$  and prioritise high-redshift candidates for spectroscopy. The fields were chosen to have the lowest possible Galactic reddening, H I column density and dust emission at 100 microns. Fields with existing multi-wavelength data were strongly preferred. Additionally, these fields had to be accessible from Chile, as they will be a natural choice for follow-up studies with ALMA.

This programme started as a collaboration between astronomers from Universidad de Chile and Yale University and now includes a total of 30 investigators from Chile, Europe and USA, plus seven Ph.D. students. The first data for this survey were obtained in October 2002 and the primary optical and near-IR imaging programmes are now finished, with follow-up spectroscopy and imaging (medium-band optical, Spitzer, sub-mm) ongoing. All data from this survey will be made public, with reduced images and catalogues already available from the broadband optical and near-IR imaging. Instructions for download of the data and more information about the survey can be found at the webpage <http://www.astro.yale.edu/MUSYC>.

## Optical imaging

Optical imaging was performed mostly using the Blanco 4-metre telescope at Cerro Tololo with the MOSAIC-II camera, which provides a field of view of  $\sim 36' \times 36'$ . Images were taken in the *UBVRiz'* filters. This filter set was chosen in order to maximise the number of independent flux measurements and the wavelength coverage. Most of the imaging in the ECDF-S field (except the *z'*-band) and the *U*-band imaging on the SDSS1030 field were done using the Wide Field Imager (WFI) on the 2.2-metre telescope at La Silla. Images in a narrow band filter centred at 500 nanometers were also obtained in each field in order to look for Lyman Alpha Emitters at  $z \sim 3$ . The ECDF-S imaging was made public by the ESO Deep Public Survey, COMBO-17, and GaBODS teams.

The location of each field together with the magnitude limits on each band is presented in Table 1. Colour images of each field combining data in the *U*, *B* and *R* filters are presented in Figure 1. A detailed description of the data-reduction techniques for the EHDF-S, which were also used for the other fields, was provided by Gawiser et al. (2006a). The 1.2 square degree optical catalogue contains 277 341 sources with a 50 % completeness limit of  $R \sim 26.5$ .

## IR imaging

Information at near-IR wavelengths is very important as these bands provide useful information for photometric redshifts and at the same time trace the rest-frame optical light at high redshift. The near-IR coverage of the MUSYC fields follows two complementary approaches. Each  $30' \times 30'$  field was covered up to a magnitude limit of  $K \sim 22$ ; this is called the 'wide' survey. Additionally, four  $10' \times 10'$  regions were observed for longer periods in *JHK* and Spitzer IRAC [3.6, 4.5, 5.8, 8.0 and 24] microns as part of the 'deep'

Field	RA	Dec	<i>U</i>	<i>B</i>	<i>v</i>	<i>R</i>	<i>I</i>	<i>z'</i>	NB500	<i>J</i>	<i>H</i>	<i>K</i>
ECDF-S	03:32:29.0	-27:48:47	26.0	26.9	26.4	26.4	24.6	23.6	25.5	24.3	23.8	23.4
SDSS1030	10:30:27.1	05:24:55	25.7	26.0	26.2	26.0	25.4	23.7	24.8	24.1	23.9	23.3
CW1255+01	12:55:40.0	01:07:00	26.0	26.2	26.1	26.0	25.0	24.1	24.4	24.0	22.8	23.0
EHDF-S	22:32:35.6	-60:47:12	26.0	26.1	26.0	25.8	24.7	23.6	24.1	24.3	23.4	23.4

**Table 1:** Optical positions and magnitude limits for each of the MUSYC fields. RA is in hours, while Dec is in degrees. Depths are  $5\sigma$  AB magnitude limits for point sources. Except in ECDF-S, the near-IR depths correspond to the 'deep' survey regions.

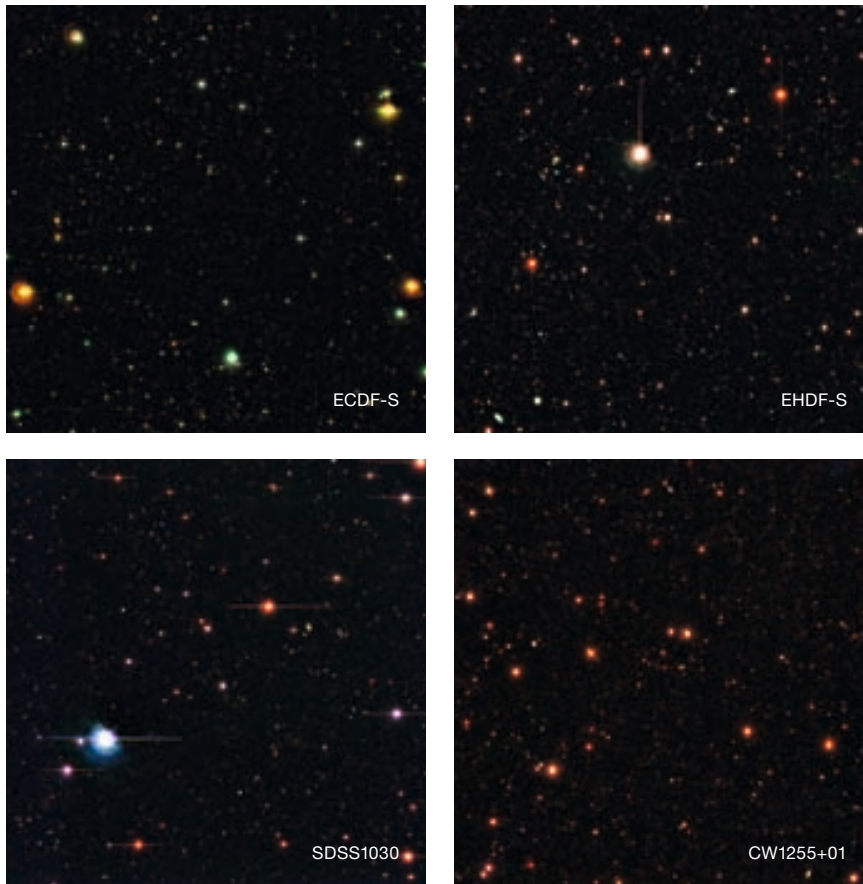


Figure 1: Optical images of the four  $30' \times 30'$  fields in the MUSYC survey.

survey. Spitzer magnitude limits are AB  $\sim 23\text{--}24$  ( $5\sigma$ ) at 3.6 and 4.5 microns and  $\sim 21\text{--}22$  at 5.7 and 8 microns, while the exposure time in the MIPS 24 micron band is  $\sim 0.5\text{--}1$  hour per field. In ECDF-S these data were taken over the full  $31' \times 31'$  field, with the Spitzer-IRAC coverage comprising a Cycle 2 Legacy Survey (SIMPLE, PI van Dokkum) and the MIPS 24 micron coverage from GTO observations (PI Riecke). The near-IR imaging was obtained using the Infrared Sideport Imager (ISPI) on the CTIO Blanco 4-metre telescope. This detector provides a field of view of  $10.5' \times 10.5'$ , one of the widest field cameras available in the near-IR. In the particular case of the ECDF-S, deep NIR coverage is provided by the GOODS survey, from data obtained using ISAAC at the VLT to depths of  $J \sim 25$ ,  $H \sim 25$  and  $K \sim 24$ . In the EHDF-S, two adjacent deep fields were

taken in order to obtain a combined deep field of  $19.5' \times 10'$ . A composite *RJK* image of one of the EHDF-S deep fields is shown in Figure 2. Additional information and a description of the data reduction can be found in Quadri et al. (2007b).

#### X-ray, UV, and radio imaging

One of our fields is the Extended Chandra Deep Field-South, which includes Chandra imaging over 1 Ms of the famous CDF-S and 250 ks over the  $30' \times 30'$  region surrounding it. The ECDF-S was also observed with XMM ( $\sim 500$  ks), with GALEX in the ultraviolet as part of their deep imaging programme, by the Hubble space telescope Advanced Camera for Surveys (ACS) as part of the GEMS and GOODS surveys, and has received deep radio coverage from VLA and ATCA. The EHDF-S is the region surrounding the Hubble Deep Field South, a well-studied region of the sky including multi-fre-

quency radio imaging by ATCA. The SDSS1030 field was observed by XMM in X-rays for a total of  $\sim 100$  ksec.

#### Spectroscopic data

An extensive spectroscopic follow-up programme is underway. Optical spectroscopy uses the multiobject spectrographs on 8-metre-class telescopes in order to efficiently reach depths comparable to our photometry. This part of the project uses the Visible Multiobject Spectrograph (VIMOS) at the VLT and the Inamori Magellan Areal Camera and Spectrograph (IMACS) on the Baade telescope at the Las Campanas Observatory. The general MUSYC spectroscopic programme uses medium-resolution grisms,  $R \sim 500$  for VIMOS and  $\sim 1000$  for IMACS, since the main goal is to provide redshifts and basic identifications. As it is not possible to obtain spectra for all sources in our fields, only a small fraction,  $\sim 5\%$ , of the sources will be targeted. Each mask contains  $\sim 100$  objects selected for specific science goals and is observed for  $\sim 3\text{--}6$  hours in order to reach a magnitude limit of  $R \sim 24$  in the continuum. Near-IR spectroscopy has been obtained for a sample of  $\sim 30$  high-redshift galaxies using VLT+SINFONI and Gemini-S+GNIRS.

Figure 2: *RJK* composite of one of the  $10' \times 10'$  deep regions in the EHDF-S. These deep near-IR observations allow for the detection of high-redshift galaxies and highly obscured sources.



## Galaxy formation and evolution

Our rich multi-wavelength data set has yielded significant advances in understanding the nature of Lyman-Alpha-Emitting galaxies (LAEs). Our narrowband imaging was used to select a sample of 162 LAEs at  $3.08 < z < 3.12$ ; spectroscopic follow-up determined precise redshifts for 60 of these objects and showed no evidence for contamination from lower-redshift emission-line galaxies (Gawiser et al. 2006b). We measured the continuum and emission-line luminosity functions and found that the LAEs have a median continuum magnitude of  $R = 27$  and very blue continuum colours, similar to those of Lyman break galaxies (LBG; see Figure 3). These blue colours and the relative strength of Lyman alpha and ultraviolet continuum emission imply very little or no dust content, consistent with these galaxies being found in the early stages of a burst of star formation. Our full SED analysis (see Figure 4) found rapid star-formation rates ( $\sim 6 M_{\odot}/\text{yr}$ ), low stellar masses ( $\sim 10^9 M_{\odot}$ ), and no evidence for a substantial AGN component (only 3/162 LAEs are detected in X-rays). The lack of ultra-high equivalent-widths, as found in  $z > 4$  LAEs, argues that the  $z \sim 3$  LAEs do not represent primordial Pop III objects.

We have also applied our multi-wavelength data to construct a stellar mass-selected sample of 294 galaxies with  $M > 10^{11} M_{\odot}$  at  $2 < z < 3$  (van Dokkum et al. 2006). 70% of this sample is comprised of the recently-discovered population of Distant Red Galaxies (DRGs) having  $J-K > 2.3$  (Vega), and only 20% have the right rest-frame UV colours to be selected as LBGs. The DRGs represent a mix of passive galaxies, with low star-formation rates (Kriek et al. 2006), and dusty active galaxies, whose 24-micron Spitzer detections imply an average star-formation rate of  $\sim 130 M_{\odot}/\text{yr}$  (Webb et al. 2006). We measured the rest-frame optical luminosity functions of  $K$ -selected galaxies at  $2 < z < 3.5$  and found a characteristic magnitude  $\sim 1.2$  mags brighter than in the local Universe, but a space density  $\sim 5$  times smaller (Marchesini et al. 2007). The DRGs dominate the stellar mass density of the Universe in this redshift range. A clustering analysis of galaxies with  $K < 21$  (Vega) found that they re-

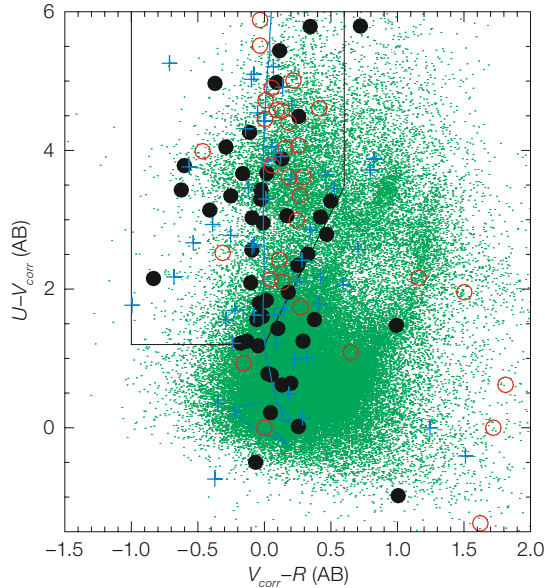


Figure 3: The  $U-V$  versus  $V-R$  colours of LAEs at  $z = 3.1$ , showing spectroscopically confirmed LAEs (solid circles), objects with insufficient signal-to-noise for spectroscopic classification (open circles), and objects without spectroscopy (crosses). The green dots show the entire 84410 objects in the optically-selected catalogue of ECDF-S. The polygon is the LBG selection region. The solid blue curve shows the track of an LBG template spectrum, which falls within this selection region at  $2.8 < z < 3.4$ . The contribution of each LAE's emission line to its  $V$ -band flux has been subtracted.

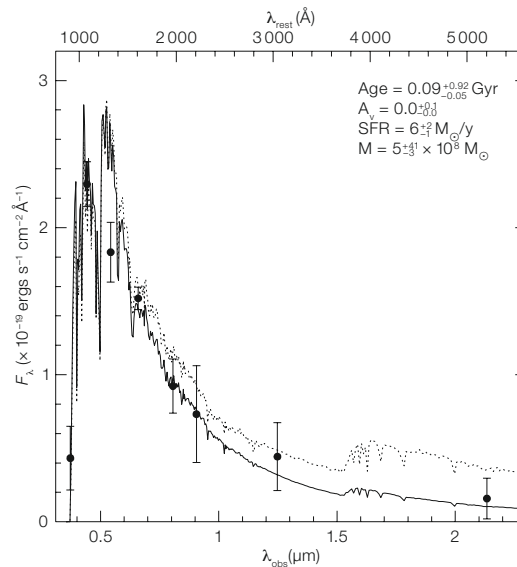


Figure 4: Average  $UBVRIZJK$  broadband photometry of LAEs from Gawiser et al. (2006b) along with best-fit model from SED fitting (solid), with model parameters listed. The dotted curve shows a maximally old model with stellar population age fixed to 2 Gyr (the age of the Universe at  $z = 3.1$ ).

side in massive dark matter halos of  $\sim 5 \times 10^{12} M_{\odot}$ , while the subset of galaxies qualifying as DRGs reside in even more massive halos of  $\sim 2 \times 10^{13} M_{\odot}$  (Quadri et al. 2007a). These halos are sufficiently massive that the typical descendants of  $K$ -selected galaxies at  $z > 2$  will reside in groups and clusters at  $z = 0$ . Several of the  $K$ -selected galaxies have been identified as potential AGN hosts based upon their  $[\text{N II}]/\text{H}\alpha$  emission line ratio, and it appears that AGN are preferentially found in the most massive galaxies at  $z > 2$  (Kriek et al. 2007).

Given the over 100 000 galaxies at  $z < 1$  on the MUSYC fields, all of them with accurate photometric redshifts and many of them with spectroscopic identifications, it is possible to study them in a statistical sense. Using data from three MUSYC fields we have found that the clustering length increases slightly from  $z \approx 0.3$  to  $z = 0.9$  while the mass of the galaxy host halos are roughly constant at a value of  $M_h = 10^{13.5 \pm 1.2} M_{\odot}$  for galaxies with  $M_R < -17$  in the same redshift range. From the GALEX ultraviolet data in the ECDF-S, we can conclude that elliptical galaxies

at  $z > 0.5$  still show a significant recent star formation, more than what was originally expected. This amount of star formation remains constant up to  $z \sim 1$ , contrary to late-type galaxies, which show an increase in the star-formation rate with increasing redshift.

### Active Galactic Nuclei (AGN)

In order to correlate the AGN activity with the properties of the supermassive black holes found in the centres of the most massive galaxies, a large unbiased sample of AGN to high redshifts is required. Surveys that rely on the optical properties of AGN (blue continuum, broad emission lines) often miss a large number of sources, those in which obscuration in the line of sight is present. In order to obtain a more complete AGN sample, X-ray and IR observations are critical, as the effects of obscuration are less important at these wavelengths. One of the MUSYC fields, the ECDF-S, was completely covered by Chandra observations. Based on the data analysis and reduction of Virani et al. (2006), 651 unique X-ray sources were found in that field. An identification programme is ongoing using IMACS and VIMOS. So far,  $\sim 250$  X-ray sources have been observed.

Combining the spectroscopic redshifts with the optical, near-IR and X-ray fluxes provides important clues about the AGN population. In Figure 5, we show the hard X-ray luminosity (in the 2–8 keV band) versus ‘Hardness ratio’ diagram. The hardness ratio, defined as  $(H-S)/(H+S)$  where H and S are the count rates in the hard and soft, 0.5–2 keV, bands, is a measure of how hard the observed X-ray spectrum is. As can be seen in that figure, the most luminous sources are in general also harder, and are also classified as unobscured AGN based on their optical properties (presence of broad emission lines). This shows that there are relatively more unobscured AGN at higher luminosities, and, as expected, these sources have softer X-ray spectra, as obscuration makes the observed X-ray spectra harder.

One very interesting class of objects are the Extreme X-ray to Optical sources (EXOs), which are defined as sources

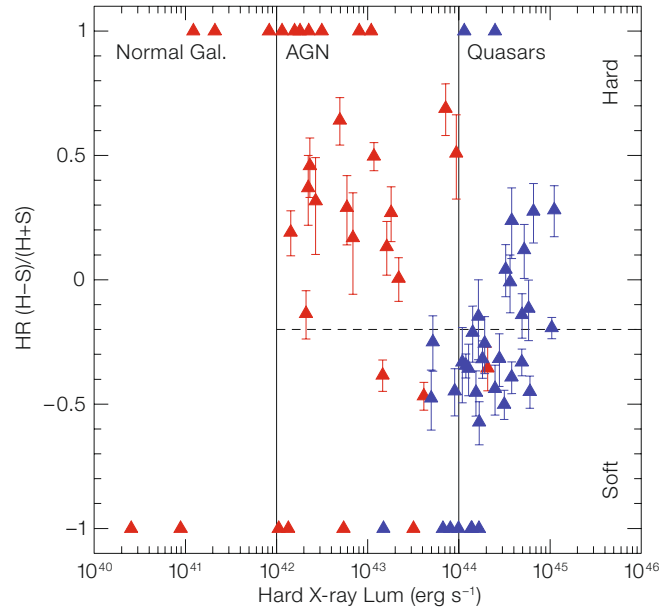


Figure 5: Hardness ratio versus hard X-ray luminosity for the sources with measured redshift in the ECDF-S. Blue symbols show the location of the sources classified as unobscured AGN based on their optical spectra (presence of broad emission lines).

with clear X-ray and near-IR detections, but no detectable optical counterpart. Two competing hypotheses have been proposed to explain these sources: either they are at very high redshift,  $z > 6$  so that the Lyman break is moved beyond the optical bands; or they are highly obscured AGN at  $z \sim 2-3$  with underluminous host galaxies. In either case, given their X-ray fluxes, these sources should host an AGN. In the ECDF-S we found 12 X-ray sources not detected in the combined *BVR* image, but clearly detected in the *K*-band image. Contrary to the sources in the CDF-S proper/GOODS-S field, which are very faint even in the near-IR bands ( $K > 21$  mag), our sources are on average brighter, with four of them having  $K < 20$  and thus follow-up studies are possible. In particular, our ongoing near-IR spectroscopy programme using Gemini-S+GNIRS and SINFONI at the VLT will provide secure redshifts and confirm the nature of these sources. Currently, no EXO has a measured spectroscopic redshift.

### The structure of our Galaxy

Unlike most deep surveys, MUSYC has been designed with Galactic science in mind. Multiple epochs of optical imaging are being used to conduct a proper-motion survey to find white dwarfs and brown dwarfs in order to study Galactic structure and the local Initial Mass Function. The Galactic programme also includes the study of stellar statistics. One of the first results was the measurement of the Galactic scale height from a sample of M and K stars selected on the basis of their photometric properties. The Galactic thick disc has a scale height of  $\sim 900$  parsecs, while the halo, which does not have an exponential distribution, has a power law fall-off coefficient of  $-3.5$  to  $-4.5$ .

### References

- Gawiser E. et al. 2006a, ApJS 162, 1
- Gawiser E. et al. 2006b, ApJ 642, L13
- Kriek M. et al. 2006, ApJ 649, L71
- Kriek M. et al. 2007, ApJ, in press, astro-ph/0611724
- Marchesini D. et al. 2007, ApJ 656, 45
- Quadri R. et al. 2007a, ApJ 654, 138
- Quadri R. et al. 2007b, AJ, in press, astro-ph/0612612
- Van Dokkum P. G. et al. 2006, ApJ 638, L59
- Virani S. et al. 2006, AJ 131, 2373
- Webb T. M. A. et al. 2006, ApJ 636, L17